April 2015

Studying Polymer Fouling in Biofuel Detoxification Membranes using Quartz Crystal Microbalance with Dissipation Monitoring

Alexander Philip Haring
Worcester Polytechnic Institute

Studying Polymer Fouling in Biofuel Detoxification Membranes using Quartz Crystal Microbalance with Dissipation Monitoring

Final Report

By: Alex Haring

Advised by: Professor Amy Peterson and Professor Michael Timko

Abstract:

Biofuel production from lignocellulosic biomass is a promising direction for reducing the global dependence on fossil fuels. One of the hindrances to industrial scale biofuel plants is achieving sustained performance of detoxification membranes. The membranes are important for removing toxic compounds that inhibit fermentation and can be sold as feedstock for renewable materials, further increasing profitability. Over time these membranes foul, resulting in decreased flux. This project aimed to develop a protocol for studying the fouling using Quartz Crystal Microbalance with Dissipation Monitoring (QCM-D), and to acquire preliminary data studying the relationship between hydrophobicity and fouling while controlling roughness. Three polymers were studied: polydimethylsiloxane (PDMS), polyamide (PA), and polyether sulfone (PES) using a model mixture containing carbohydrates and carbohydrate decomposition products. The chosen polymers have been used previously as detoxification membranes and exhibit a suitable range of hydrophobicity. Hydrophobicity was characterized by static water contact angle and roughness was characterized by AFM. Control and reproducibility studies established a reliable protocol for obtaining polymer fouling data for PES and PA; experiments with PDMS failed possibly due to a lack of adhesion of the membrane to the QCM-D sensor. Specifically, reproducible protocol requires gentle heating and filtering of the test solution and careful climate-controlled storage of the polymer before testing. Using the optimized protocol, the QCM-D revealed that the polymers acquired between 1405 and 2010 ng/cm^2 of mass during a 10 hour exposure. Surprisingly, laboratory temperature played a strong role in the mass uptake results. Under all cases, mass accumulated rapidly on the polymer membrane during the initial 30 min of exposure time, followed by a more gradual increase over the next 9.5 hours. The experimental data showed a potential relationship between hydrophobicity and increased fouling, though increased data are required especially for highly hydrophobic materials such as PDMS. Future work should continue to refine the established protocol; expand the study to consider a wider range of chemical and physical polymer properties; and couple QCM-D studies with engineering studies of membrane permeation and selectivity.

1. Introduction

As the world pushes to reduce its dependence on petroleum based fuels, biofuels are being studied as a viable alternative. Biofuels have a number of advantages over traditional fossil fuels. The CO_2 released in the burning of biofuels is CO_2 that was recently removed from the atmosphere by plants, so it will not cause a significant increase in atmospheric CO_2 levels. Additionally, biofuels are produced from biomass that can be managed and quickly replenished [1]. In fact, some models predict that biofuels will make up 50% of the world's energy usage by 2050 [1]. However, the economics of biofuel production must be improved to make a shift in fuel usage achievable.

Producing biofuels through hydrolysis and fermentation of lignocellulosic biomass is one of the most promising directions currently being studied. The acetone-butanol-ethanol (ABE) fermentation is of particular interest given the superior fuel characteristics of butanol compared to ethanol. Additional methods of producing biofuels include gasification and pyrolysis [2], but hydrolysis and ABE fermentation are the focus of this project. Ethanol and butanol are promising biofuels because both are promising substitutes for gasoline and other petroleum-based fuels [3]. The basic biofuel production process consists of pretreatment of corn stover or sweet sorghum, followed by enzymatic hydrolysis, detoxification, ABE fermentation, and finally purification. For biofuels to become widely produced, each of these steps must be optimized for efficiency and profitability.

Membranes are of interest for removal of fermentation inhibitors in the detoxification step. Not only do these toxic compounds inhibit fermentation, but some of these compounds, such as furfural, are high value chemicals that could increase the profitability of a biofuel process [4]. Pervaporation membranes have been identified relatively recently as the most energy efficient technique to carry out this separation [5]. However, fouling has been observed as a problem and must be studied and hopefully minimized before membrane use will be feasible in a large scale biofuel process [6-8]. While the flux and selectivity of these membranes have been rigorously assessed for performance in biofuel processing, little has been done to study fouling.

Several reports assessing the performance of these membranes have mentioned fouling as a problem for sustained performance [1, 11]; however, very few discuss the problem in detail [7, 8]. One recent study assessed the fouling problem on polyamide and poly(piperazine-amide) membranes by monitoring the decrease in flux over time [7]. This study provided quantitative evidence of the fouling problem and identified surface roughness, hydrophilicity, and porosity as factors that may contribute to fouling; however, the study was not able to separately evaluate the effect of each of these parameters.

This MQP sought to test the hypothesis that membrane hydrophilicity contributes to fouling. This was achieved by studying fouling of polymers commonly used for membranes using a quartz crystal microbalance with dissipation monitoring (QCM-D). As a substantial first step, a protocol

for studying membrane surface fouling using QCM-D was developed, which can be used for future studies. A model solution was created in the lab with similar compositions to actual cellulose hydrolysates. The polymers were spin coated onto the quartz disks and annealed above their glass transition temperature (T_gs) to control roughness. The roughness of each sample was quantified by atomic force microscopy (AFM). Hydrophilicity was characterized by static water contact angle.

2. Background

2.1. Overview of the Biofuel Production Process

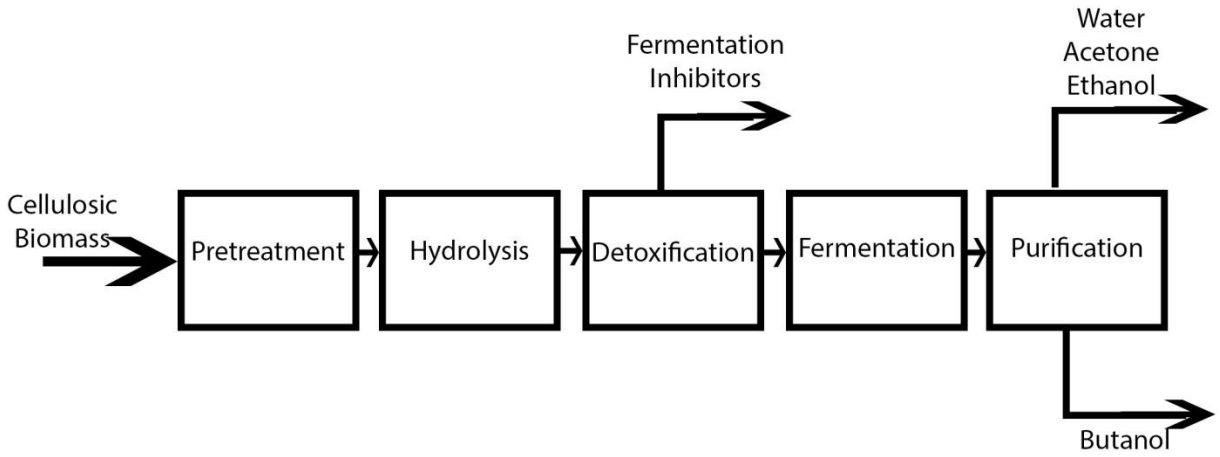

Figure 1. Block flow diagram of the production of biofuels from cellulosic biomass through hydrolysis and ABE fermentation.

The first step in the production of biofuel from lignocellulosic biomass is pretreatment. The purpose of pretreatment is to break down the lignin into phenolic alcohols and hemicellulose into sugars and furan derivatives, as well as to disrupt the crystal structure of cellulose [9]. This step is necessary to prepare the biomass for enzymatic hydrolysis and fermentation. Pretreatment is possibly the most expensive step in the process, and there is much room for improvement. The pretreatment can be mechanical, chemical, electrical, biological, or a combination of multiple methods. One of the more common pretreatment techniques is the use of dilute sulfuric acid. Sulfuric acid is added to the biomass, usually below 4% concentration and at temperatures above 160 °C. Pretreatment by dilute sulfuric acid is advantageous because it can break down close to 100% of the hemicellulose in the biomass. Additionally, the sulfuric acid will break down xylose into valuable byproducts such as furfural [10].

Byproducts of pretreatment can inhibit fermentation, so a detoxification step is necessary. Separation of these inhibitors is economically desirable as well; furans are valuable chemical solvents and base chemicals for synthesis. Membrane pervaporation is a cost effective separation process that has been gaining interest recently. Several membranes such as polydimethylsiloxane (PDMS), polyamide (PA), polyethersulfone (PES), and polypropylene (PP) have been tested for

the detoxification of lignocellulosic hydrolysates [3, 4, 11]. Specifically, furfural, 5-hydroxymethylfurfural (HMF), acetic acid, levulinic acid, formic acid, and phenolic fragments of lignin need to be removed to allow fermentation to take place [12]. Studies have proven that membrane extraction can be an effective method for removing these inhibitors, and fermentation of hydrolysate detoxified by pervaporation is possible [3, 4, 11, 13].

In ABE fermentation the microorganisms can only break down monomeric sugars, so the cellulose must by hydrolyzed. Hydrolysis can be carried out before, simultaneously, or after the detoxification step [12]. Enzymatic hydrolysis is the preferred method for hydrolyzing cellulose, however acid-catalyst hydrolysis is another option [12, 14]. In enzymatic hydrolysis, an enzyme from the cellulase family is used for the decomposition of cellulose. The disruption of crystallinity in the pretreatment step is critical, because amorphous cellulose can be hydrolyzed 30% faster than crystalline cellulose [15]. Depending on the type of cellulase used and the reaction conditions, the composition of the hydrolysate will vary. Cellulose hydrolyzes into a variety of simple sugars such as glucose, xylose, and arabinose, as well as disaccharides such as cellobiose and sucrose [3, 15].

After pretreatment, detoxification, and hydrolysis, the next step is fermentation. Microorganisms are used to digest the sugars in the hydrolysate creating acetone, butanol, and ethanol. The strains in the *Clostridium* genus are the most commonly used butanol-producing microorganisms [16]. Because of its ability to be used as a replacement for automotive or aviation fuels with little to no modification to the engine, butanol is the preferred product of fermentation [3]. Genetic mutation of strains such as *C. acetobutylicum* and *C. beijerinckii* are hyperbutanol-producing because of the high concentration of butanol in the product with little to no acetone. These mutant strains also have higher tolerances for fermentation inhibitors: *C. acetobutylicum* will tolerate 15 g/L acetic acid and 4 g/L furfural or HMF

Following fermentation is the final step in the biofuel production process: separation and purification. Due to its importance for the profitability of the process as well as the viability of the product as a fuel, this has been a major area of research and many different operations have been studied: gas stripping, vacuum flash, liquid-liquid extractions, membrane perstraction, membrane distillation, membrane pervaporation, thermovaporation, reverse osmosis, and adsorption [17]. Membrane pervaporation has been established as the most efficient operation, and current designs can achieve up to 82.9 wt.% butanol with relatively low energy requirements [17]. It has also been shown that a PDMS membrane can be used for both the detoxification step and the separation step [3].

2.2. Current Understanding of the Fouling Problem

Fouling is apparent when the flux across the membrane decreases over time, and this has been observed in hydrolysate systems [6-8]. Lignan has been identified as one of the main fouling agents, so breaking more down during pretreatment could improve membrane performance [8]. Membrane characteristics such as low hydrophilicity, low porosity, and high surface roughness

have been identified as characteristics of highly fouling membranes [7, 8]. Differences in fouling between real hydrolysate samples and laboratory produced sugar solutions have been noticed and are important for experimental design [7].

A recent article from Guatam and Menkhaus [7] performed on polyamide and poly(piperazine-amide) revealed that a portion of the fouling was reversible and could be removed by flushing with water. With model sugar solutions, 43% of the fouling was reversible on average in reverse osmosis (RO) membranes and 68% of the fouling was reversible on nanofiltration (NF) membranes [7]. Using real enzymatic hydrolysates, 30% of the fouling on RO membranes was reversible and 33% of the fouling on NF membranes was reversible [7]. The lower levels of reversible fouling in the hydrolysate samples are due to a lower total concentration of sugars in the retentate when compared to the model sugar solution. This reversible fouling likely consists of deposited solids and caked on sugars. The irreversible fouling was not entirely understood; however, it was noted that the membranes that collected phenolic compounds in the permeate showed less irreversible fouling [7]. The Guatam and Menkhaus study [7] clearly establishes the potential for biofuels separations using polymer membranes and points to fouling as a crucial literature gap.

2.3. Quartz Crystal Microbalance with Dissipation Monitoring (QCM-D)

The heart of the QCM-D is a sensor comprised of a 14 mm quartz disk with gold electrodes. The electrodes force the sensor to vibrate at its resonance frequency, which is monitored. A solution is pumped across the sensor contained inside a flow module. As mass accumulates on the sensor, the resonance frequency will decrease and dissipation will increase. The drop in frequency is used to measure the change in mass, while the dissipation is used to determine the rigidity of the additional mass. The QCM-D can accurately measure changes in mass on the nanoscale [18]. QCM-D has been used for a number of applications, including studying fouling on polymeric membranes [19,20]. Studies on extracellular polymeric substance fouling on polyvinylidene fluoride (PVDF) and surfactant fouling on PES have proven that QCM-D is an appropriate technique for characterization of fouling [19, 20].

3. Methodology

3.1. Materials

Polymers:

- Polyamide (PA) from BASF as Ultramid B
- Polyethersulfone (PES) from BASF as Ultrason E 2020 P
- Polydimethylsiloxane (PDMS) from Dow as Sylgard 184

Spin-casting Solvents:

- n-heptane for PDMS

- benzyl alcohol for PA
- N,N-Dimethylacetamide (DMAC) for PES

Model Solution:

A model solution was created in the lab to simulate a lignocellulosic hydrolysate with controlled composition. It was an aqueous solution containing glucose, hydroxymethylfurfural (HMF), cellobiose, and syringol. These compounds were chosen so that the solution would contain one monosaccharide, one disaccharide, one furan derivative, and one phenolic compound. In a real lignocellulosic hydrolysate the glucose and cellobiose would be produced by the hydrolysis of cellulose, the HMF would be produced from hemicellulose and cellulose during the pretreatment step, and syringol would be produced from the breakdown of lignin in the pretreatment step. The exact composition of cellulose hydrolysates can vary greatly depending on the biomass used, the pretreatment method, and the hydrolysis conditions [15]. The model solution was created based on typical concentrations of sugars and inhibitors, with 80% of the dry weight as sugar and 80% of the sugars as monomers: 19.2 g/L glucose, 4.8 g/L cellobiose, 3 g/L HMF, and 3 g/L syringol. The solution was stored in a refrigerator.

Component	Dry wt. % in Solution	Concentration (g/L)	Water Solubility (g/L)
Glucose	64%	19.2	909
Cellobiose	16%	4.8	1950
5-Hydroxymethylfurfural	10%	3	364
Syringol	10%	3	7.58

Figure 2. Model hydrolysate solution composition and water solubility of components

3.2. Production of Samples

Polished quartz disks (25 mm diameter) were sputter coated with gold to replicate the surface of the QCM sensors. Each polymer was spin coated onto three of the quartz disks, for a total of nine replica sensors. PES was dissolved in DMAC at room temperature, and Polyamide was dissolved in benzyl alcohol at 130 °C. The PDMS base and curing agent were dissolved in n-heptane. The disks were spun at 2000 rpm for 1 minute. The samples were then annealed above their T_gs to remove the roughness contribution from spinning and to conform to the surface of the gold substrate. Due to PDMS's low T_g (-50°C) it required no additional steps and remained at room temperature. However, the PDMS coated sensors were allowed to cure for 72 hours before testing. Polyamide was annealed for 30 minutes at 75 °C. Polyethersulfone was annealed at 250 °C for 10 minutes. This shortened annealing time was chosen to prevent chromium in the adhesive layer of the QCM-D sensors from migrating into the gold. These quartz disks were used to characterize the surface roughness and contact angle of each polymer. The same protocol was used to spin coat the QCM-D sensors.

3.3. Characterization of Surface Roughness

Surface roughness was characterized for each sample using an atomic force microscope (AFM). The naioAFM located in Olin Hall was used. The scans were conducted at a rate of 1 s/line with a resolution of 256 pixels/line, and a scan range of 5 μm. For the PES and PA samples HQ:CSC17 cantilevers were used in constant-force contact mode with a set-point force of 55 nN. The PDMS surfaces were too compliant to acquire clear images using the naioAFM. The ability to control and quantify surface roughness allowed us to look at the relationship between polymer fouling and hydrophilicity with minimal effect from differing surface roughness.

3.4. Characterization of Hydrophobicity

Hydrophobicity was characterized by measuring the static water contact angle. Static contact angle is the angle at the interface between a drop of liquid and a solid surface. If there is a strong attraction between the liquid and the surface, the drop will spread out and decrease the contact angle; this is called wetting. If there is repulsion between the liquid and the solid, the contact area between the drop and the surface will decrease, resulting in a larger contact angle. The contact angles for this project were measured using the Rame-Hart Contact Angle Goniometer located in the Life Sciences and Bioengineering Center. When water is used as the liquid, a contact angle less than 90° indicates a hydrophilic surface, while a contact angle greater than 90° is formed on hydrophobic surfaces [21]. The contact angle on each coated quartz disk was measured three times, yielding nine measurements for each polymer. Hydrophobicity has been identified as a contributing factor to fouling [7], and quantifying it through contact angle measurements allowed for this relationship to be studied.

3.5. Monitoring Fouling through QCM-D

Fouling on the polymer coated sensors was monitored using a Biolin Scientific Q-Sense E4 QCM-D. This QCM-D model allowed four tests to be carried out in parallel. The resonance frequencies of each sensor were measured in air before testing, making sure that the results had not changed significantly from previous experiments. Changes in the resonance frequencies could indicate a damaged sensor. After finding the resonance frequencies in air, DI water was pumped through the system at the testing conditions of 40 °C at a rate of 50 μL/min. The volume above the sensor is 40 μL, which yields a residence time of 48 seconds. Once the frequencies leveled out in water and a baseline was acquired, the model solution was pumped through the QCM-D at the same temperature and flow rate. In a rigid system, changes in frequency are correlated to changes in mass using the Sauerbrey equation:

$$\Delta f = -\frac{2f_0^2}{A\sqrt{\rho_q \mu_q}}\Delta m \qquad (1)$$

Where Δf is the change in frequency, Δm is the change in mass, f_0 is the fundamental frequency, A is the area, ρ_q is the density of quartz, and μ_q is the shear modulus of quartz. Fouling tests were run for approximately10 hours. Data was collected for five tests of each polymer. On 3/19/15 and 3/23/15, solutions were pre-heated to 40°C before entering the QCM-D chamber. Four of the tests

were conducted with a model solution filtered through a 0.2 μm PTFE filter these tests are labeled as filtered in the results. After the tests were finished the polymer coating was removed with the appropriate solvent and the sensors were cleaned using "Protocol A-1", and each module was cleaned using "Protocol Daily". Sensors were re-coated and reused after cleaning. The cleaning protocols can be found in the appendix figures A-12, A-13, and A-14.

3.5 Qualitative HPLC Study

HPLC was used to gain a better understanding of which component or components of the hydrolysate are fouling. The HPLC study was not designed to be quantitative, and instead was focused on identifying relative changes in concentrations of specific biofuel components before and after exposure to the membrane. The original model solution was tested, as well as solutions that had been run through QCM-D with PES and PA. The QCM-D was run in parallel mode so the effluents could be split and only came in contact with one sensor. The tests were conducted by a graduate student, Max Tyufekchiev, on a Shimadzu HPLC. The HPLC set up is described below:

Column: Phenomenex Rezes ROA-Organic Acid H+(8%), 300x7.8 mm

UV detector: Shimadzu SPD-10A UV/Vis Detector, 285 nm

ELSD: Shimadzu Sedex 75

Settings: 0.6 mL flow; 0.00035 M H_2SO_4 mobile phase; scan time 60 min

4. Results

4.1 Contact Angles

Three contact angles were measured on each quartz disk, yielding a total of nine contact angles for each material. All of the measured angles are available in Table A-1 in appendix A. The average contact angle for each polymer is shown in the table below.

Material	Contact Angle (°)
PDMS	103.3±3
PES	80.3±5
PA	46.7±2

Figure 3. Static Water Contact Angles

PDMS was the only hydrophobic polymer tested. PES was slightly hydrophilic, and PA was strongly hydrophilic. Covering this wide range of hydrophobicity allowed the effect of surface chemistry on fouling to be studied thoroughly.

4.2 Surface Roughness

4.2.1 Polyamide

A replica sensor spin coated with PA and annealed at 75 °C for 30 minutes was characterized using AFM. The z-axis scan is shown in Figure 4 below. The root-mean-squared (RMS) roughness of the PA surface was 3.3 nm.

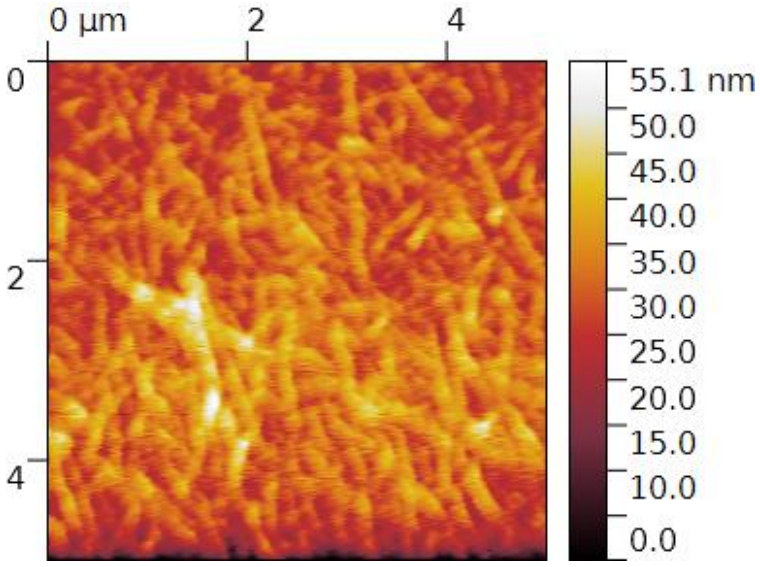

Figure 4. Z-axis AFM image of Polyamide coated replica sensor with a scan range of 5 µm.

4.2.2 Polyethersulfone

A replica sensor spin coated with PES and annealed at 250 °C for 10 minutes was scanned with the naioAFM. The z-axis constant-force contact mode scan is shown in Figure 5 below. The RMS roughness was 0.7 nm. This is only 2.6 nm less than the RMS roughness of PA, which shows good control of roughness and successful removal of the roughness effects of spin coating.

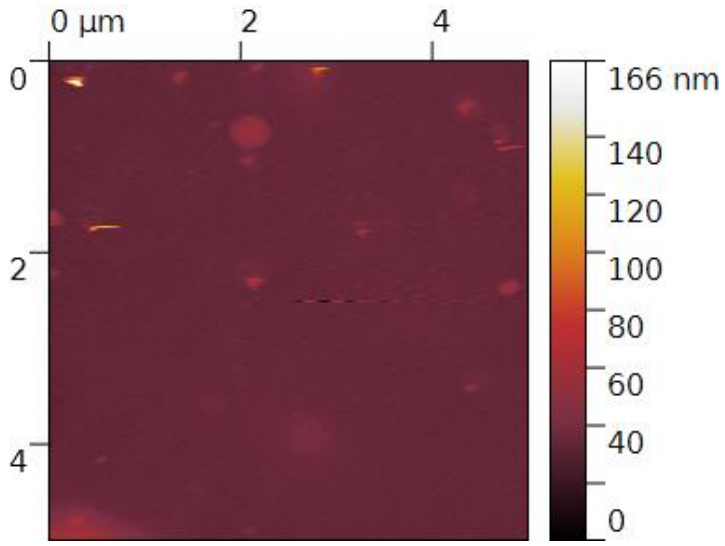

Figure 5. The z-axis constant-force contact mode AFM image of polyethersulfone.

Component	**Contact Angle**	**RMS Roughness (nm)**
Polyamide	46.7±2°	3.3
Polyethersulfone	80.3±5°	0.70
Polydimethylsiloxane	103.3±3°	N/A

Figure 6. Surface characterization results for PA, PES, and PDMS.

4.3 QCM-D Results

4.3.1 Polyamide

The QCM-D results for the polyamide coated sensors are shown in Figure 7 below. All tests yielded a rapid drop in frequency in the beginning of the test, followed by a slower decrease in frequency for the duration of the experiment. The Sauerbrey Equation was used to convert the frequency drop into increase in mass. On 2/22/15 and 2/25/15 the laboratory was much colder with temperatures as low as 8 °C than on 3/5/15, and on 3/19/15 the solution was heated to 40 °C prior to entering the QCM chamber. The data suggested an unexpected temperature dependence since the three colder days resulted in lower total fouling: 732 ng/cm^2, 502 ng/cm^2, and 360 ng/cm^2. The higher ambient temperature and preheated results converged to higher masses: 1471 ng/cm^2, 1634 ng/cm^2, and 1466 ng/cm^2. The sawtooth shape 2/25/15 (gray) was likely not a physical result, but the shape was difficult to interpret given the current data set.

The results on 3/5/15 show a peak after the initial quick increase in mass, followed by a brief decrease in mass before beginning to slowly increase for the duration of the test. The filtered result on 3/19/15 displays a similar peak mass before decreasing and slowly leveling out over time. These results may suggest two dynamic fouling regimes.

The unfiltered test on 3/19/15 (red) indicates a damaged sensor. QCM-D sensors become damaged over time, but the exact number of uses depends greatly on the test conditions. These sensors had been used four times each on 3/19/15. Two likely causes of the damage to the sensors was incomplete removal of PA during cleaning, or damage to the sensors occurring during the spin coating/annealing process. The step in the data on 3/5/15 (green) was likely due to the tubing being accidentally bumped in the lab, or a particulate in the solution causing a point force on the sensor and is not a physical result. One test has been omitted from 2/25/15, as the data was compromised likely due to a bubble on the sensor. These data are provided in Figure A-10 of the appendix. According to the QCM-D manual, differences in temperature between the testing chamber and the solution temperature can lead to formation of bubbles inside the module, so the use of a hot plate to pre-heat the solution to the sensor temperature should reduce the risk of bubble formation occurring in future tests.

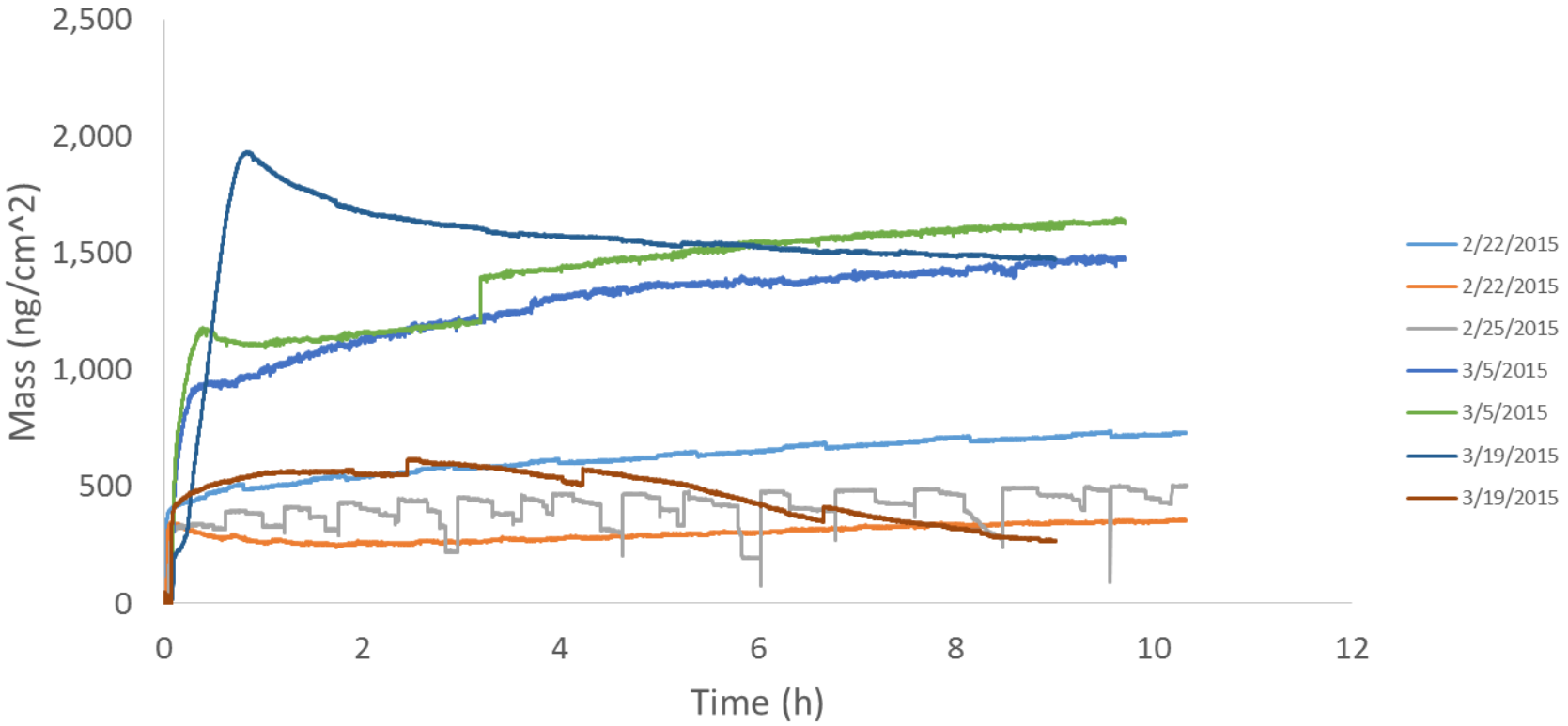

Figure 7. QCM-D results for polyamide coated sensors

4.3.2 Polyethersulfone

The QCM-D results for polyethersulfone (PES) are shown in Figure 8 below. Similarly to the polyamide (PA) results, the PES results showed a rapid initial increase in mass followed by a slower continuous increase. The test on 3/19/15 used a model solution pre-heated to the test temperature. The same temperature dependence was visible in the PES results as with the PA results; less fouling on colder days in the laboratory (2/22/15 and 2/25/15) and increased fouling on warmer days (3/5/15) or when using pre-heated solution (3/19/15). The total mass on colder days was 876 ng/cm^2, 796 ng/cm^2, and 737 ng/cm^2. The final mass on warmer days was 1405 ng/cm^2, 2010 ng/cm^2, 1427 ng/cm^2.

A sawtooth response similar to what was seen with PA on 2/25/15 was visible on 2/22/15 and 2/25/15 in the PES results. Again, at this point no conclusion can be drawn about the cause of this behavior. In the data collected, the sawtooth function only existed on days that were colder in the laboratory.

The results from the two PES tests performed on 3/5/15 initially followed almost identical trends to one another for the first 3.5 hours, at which point one of the samples rapidly stepped to a significantly greater mass. This 500 ng/cm^2 increased occurred at the same time as the step previously mentioned in the PA data, reinforcing the idea that the tubes or the lab bench were bumped; accordingly, this step is not interpreted as a physical result. Following the step, the two PES tests performed on 3/15/15 continued to follow similar slopes as one another, consistent with a brief departure followed by resumption of normal operation. The final mass of the "blue" 3/5/15 result was 1405 ng/cm^2, and the measured final mass for the "green" result was measured at 2010 ng/cm^2. If the 500 ng/cm^2 step is subtracted from the "green" test, then the two data sets agree to within 10% (1506 ng/cm^2 compared to 1405 ng/cm^2), suggesting that the data may be more repeatable than suggested by the final masses alone.

The "blue" result on 3/19/15 yielded a higher initial peak mass than any of the other tests, but decreased over time and leveled out to a similar mass as 3/5/15. This peak shape is not visible in any of the other PES results. The reason for this higher initial peak is unclear, and collecting more data will reveal if this result continues to occur.

Two tests were omitted from the PES results, and the data can be found in Figure A-11 in the appendix. An omitted test from 2/25/15 may have had a bubble, and an omitted test from 3/19/15 is consistent with a damaged sensor.

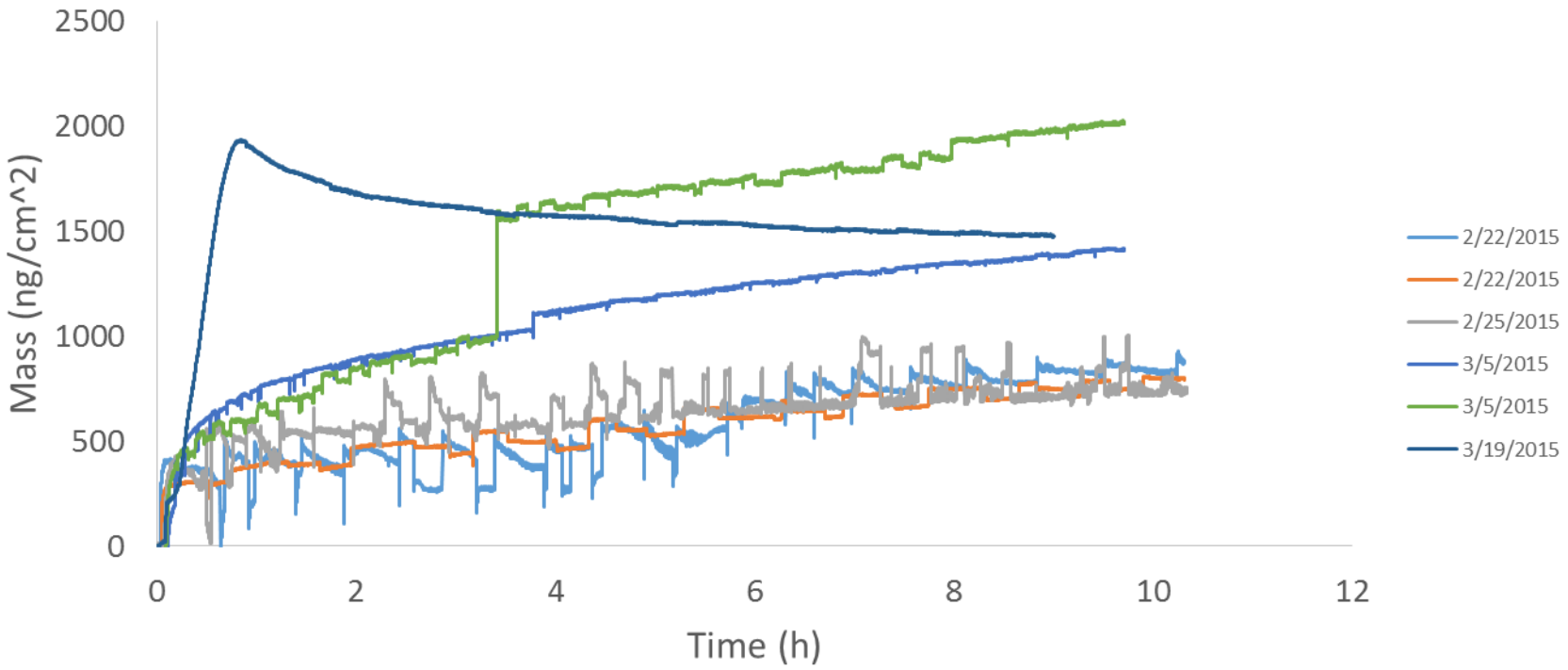

Figure 8. QCM-D results for polyethersulfone coated sensors

4.3.3 Polydimethlysiloxane

The QCM results for PDMS are shown in Figure 9 below. All tests were conducted on 3/23/15 with a hot plate pre-heating the solutions to 40 °C. Two of the tests (blue, orange) used filtered solutions and two (gray, yellow) used unfiltered solution. As shown in Figure 9, the QCM-D data for PDMS are highly inconsistent and often correspond to an apparent loss of mass, rather than the expected gain. The data may suggest that the PDMS was being removed during the test, which was supported by a visible change in the surface of the PDMS film. No conclusions about PDMS fouling can be drawn from this data.

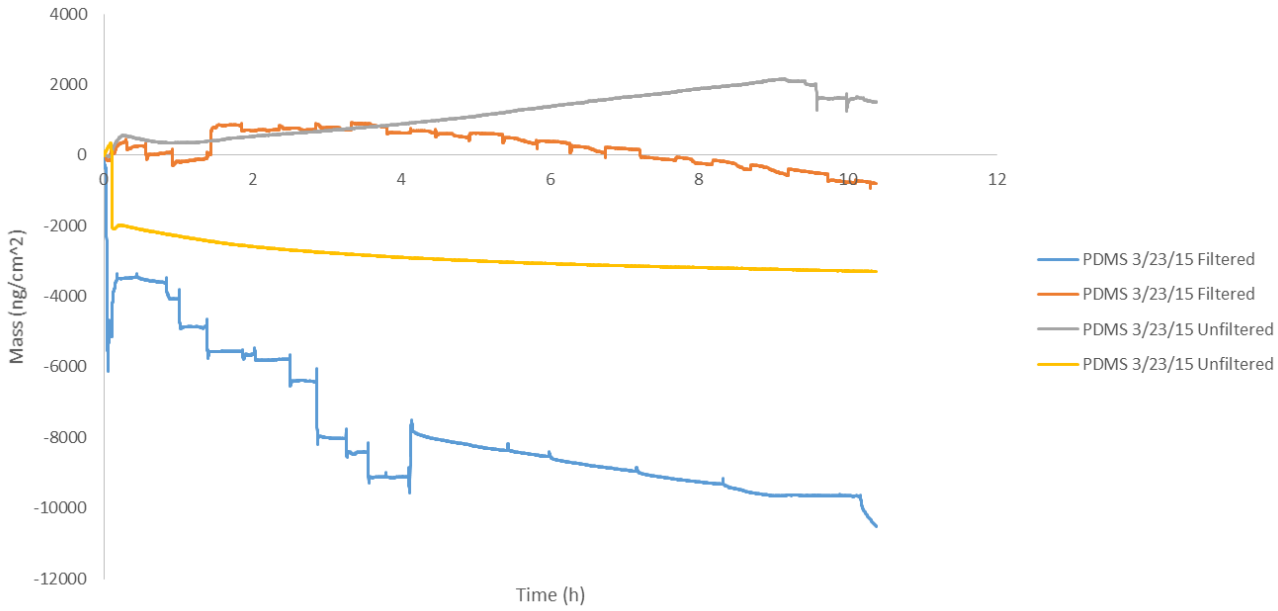

Figure 9. QCM results for polydimethylsiloxane coated sensors

4.3.4 Comparing the Polymers

The final mass accumulated on the sensors was averaged and separated by hot and cold days, shown plotted against the corresponding contact angle in Figure 10 below. The PDMS data were not included due to the poor quality of the QCM-D data. The large range and small number of data points make it difficult to draw any significant conclusions from this plot, but future studies could use a similar format to assess the dependence of fouling on hydrophilicity.

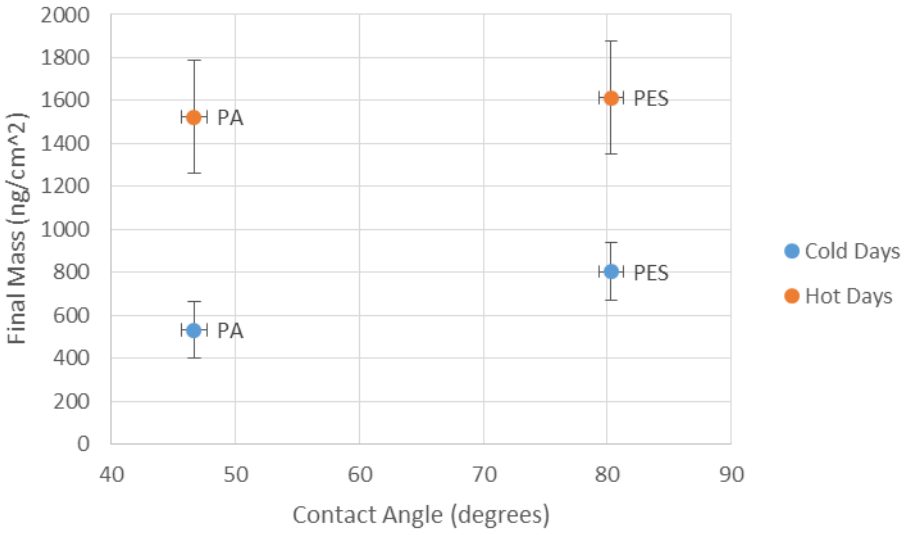

Figure 10. Average final mass of the sensors vs water contact angle, separated by hot and cold days

4.4 HPLC Results

The UV sensor shows the HMF peak at a retention time of 38.5 minutes and the syringol peak at 14 minutes. The UV sensor results were split into two graphs, one from 0-30 min, and one from 30-60 min because the HMF peak is so high that the syringol peak is difficult to see. The evaporating light scattering detector (ELSD) shows the glucose peak at 9.8 min and cellobiose at 8 min. The HPLC results for the control sample, as well as the effluent samples, are shown in Figures A1-9 in appendix A. No difference between the control and effluent samples was observed. This indicates that the amount of the solution components being deposited on the surfaces was negligible in comparison to the solution concentration.

5. Conclusions and Recommendations

This MQP leads to a better understanding of a systematic QCM-D protocol for evaluating membrane fouling and provides some insight on factors that may influence polymer membrane fouling when subjected to a biofuel intermediate stream. The project showed that the fouling problem may be more complex than originally predicted, and opened pathways for future study. A strong effect of solution temperature was observed and controlled using a hot plate. PDMS may have been removed from the gold surface during QCM-D testing, which needs to be addressed before PDMS fouling can be studied using QCM-D. The AFM results showed that annealing the polymers above their T_gs successfully removed the effects of spin coating on surface roughness. The HPLC performed in the project did not reveal which component or components were fouling, so no information on which components contribute predominantly to fouling could be obtained.

Annealing is recommended to use in further research to minimize surface roughness effects resulting from spin coating. The results showed the mass deposited on the sensors continued to increase steadily until the test was stopped; increasing the duration of the test may show if the fouling reaches a maximum. The QCM-D should be kept isolated in the future, to prevent accidental disturbances. In future work, the QCM-D technique might be used with individual hydrolysate components in solution to determine which components contribute to fouling.

References

[1] Tekin, K., Karagoz, S., and Bektas, S., 2014, "A review of hydrothermal biomass processing," Renewable and Sustainable Energy Reviews, Elsevier Ltd.

[2] Huber, G., Iborra, S., and Corma, A., 2006, "Synthesis of transportation fuels from biomass: chemistry, catalysts, and engineering," Chemical Reviews, American Chemical Society.

[3] Cai, D., Zhang, T., Zheng, J., Zhen, C., Wang, Z., Qin, P.-y., and Tan, T.-w., 2013, "Biobutanol from sweet sorghum bagasse hydrolysate by hybrid pervaporation process," Bioresource Technology, Elsevier Ltd.

[4] Grzenia, D., Schell, D., and Wickramasinghe, R., 2012, "Membrane extraction for detoxification of biomass hydrolysates," Bioresource Technology, Elsevier Ltd.

[5] Yen, H.-W., Lin, S.-F., and Yang, I.-K., 2012, "Use of poly(ether-block-amide) in pervaporation coupling with a fermentor to enhance butanol production in the cultivation of Clostridium acetobutylicum," Journal of Bioscience and Bioengineering, Elsevier ltd.

[6] Abel, M., Szabo, G., Poser, O., Laszlo, Z., and Hodur, C., 2013, "Enzyme recovery and fouling mitigation by ultrasound-enhanced ultrafiltration," Desalination and Water Treatment, Taylor & Francis.

[7] Guatam, A., and Menkhaus, T., 2014, "Performance evaluation and fouling analysis for reverse osmosis and nanofiltration membranes during processing of lignocellulosic biomass hydrolysate," Journal of Membrane Science, Elsevier Ltd.

[8] Koivula, E., Kallioninen, M., Preis, S., Testova, L., Sixta, H., and Manttari, M., 2011, "Evaluation of various pretreatment methods to manage fouling in ultrafiltration of wood hydrolysates," Separation and Purification Technology, Elsevier Ltd.

[9] Mosier, N., Wyman, C., Dale, B., Elander, R., Lee, Y., Holtzapple, M., and Ladisch, M., 2005, "Features of promising technologies for pretreatment of lignocellulosic biomass," Bioresource Technology, Elsevier Ltd.

[10] Kumar, P., Barrett, D., Delwiche, M., and Stroeve, P., 2009, "Methods for pretreatment of lignocellulosic biomass or efficient hydolysis and biofuel production," Industrial & Engineering Chemistry Research, American Chemical Society.
[11] Grzenia, D., Schell, D., and Wickramsinge, R., 2009, "Detoxification of biomass hydrolysates by reactive membrane extraction," Journal of Membrane Science, Elsevier Ltd.
[12] Bower, S., Wickramasinghe, R., Nagle, N., and Schell, D., 2008, "Modeling sucrose hydrolysis in dilute sulfuric acid solutions at pretreatment conditions for lignocellulosic biomass," Bioresource Technology, Elsevier Ltd.
[13] Malmali, M., Stickel, J., and Wickramasinge, R., 2014, "Sugar concentration and detoxification of clarified biomass hydrolysate by nanofiltration," Separation and Purification Technology, Elsevier Ltd.
[14] Kupiainen, L., Ahola, J., and Tanskanen, J., 2014, "Kinetics of Formic Acid-catalyzed Cellulose Hydrolysis," Bioresources, 9(2), pp. 2645-2658.
[15] Zhang, Y.-H., and Lynd, L., 2004, "Toward an Aggregated Understanding of Enzymatic Hydrolysis of Cellulose: Noncomplexed Cellulase Systems," Biotechnology and Bioengineering, Wiley InterScience.
[16] Schiel-Bengelsdorf, B., Montoya, J., Linder, S., and Durre, P., 2013, "Butanol fermentation," Environmental Technology, Taylor & Francis Group.
[17] Hua-Jiang, H., Ramaswamy, S., and Liu, Y., 2014, "Separation and purification of biobutanol during bioconversion of biomass," Separation and Purification Technology, Elsevier Ltd., pp. 513-540.
[18] Jaiswal, A., 2014, "QCM-D Basic Training Introduction and Application," Biolin Scientific.
[19] Liu, S., and Kim, J.-T., 2009, "Study of adsorption kinetics of surfactants onto polyethersulfone membrane surface using QCM-D," Desalination, Elsevier Ltd, pp. 355-361.
[20] Sweity, A., Ying, W., Ali-Shtayeh, M., Yang, F., Bick, A., Oron, G., and Herzeberg, M., 2011, "Relation between EPS adherence, viscoelastic properties, and MBR operation: Biofouling study with QCM-D," Water Research, Elsevier Ltd, pp. 6430-6440.
[21] Forch, R., Schonherr, H., and Jenkins, T., 2009, Surface Design: Applications in Bioscience and Nanotechnology, Wiley-VCH.

Appendix A.

Table A-1. Water Contact Angle Measurements

Material	Disk	Left	Right	Mean
PDMS	1	99.5	99.7	99.6
PDMS	1	101.7	101.8	101.7
PDMS	1	103.9	103.4	103.7
PDMS	2	106.6	104.1	105.3
PDMS	2	108.1	104.5	106.3
PDMS	2	108.9	106.1	107.5
PDMS	3	102.8	100.5	101.6
PDMS	3	102.6	101.8	102.2
PDMS	3	102.2	102	102.1
PES	1	77.2	75.9	76.5
PES	1	79.4	78.3	78.9
PES	1	76.8	75.7	76.2
PES	2	81.2	77.8	79.5
PES	2	87.5	80.3	83.9
PES	2	69.2	74.8	72
PES	3	87.9	88.1	88
PES	3	89.1	90.6	89.9
PES	3	84.7	81.2	83
PA	1	48.7	48	48.3
PA	1	45.8	46.8	46.3
PA	1	47.5	49.2	48.3
PA	2	47.9	46.2	47.1
PA	2	45.4	45.4	45.4
PA	2	42.8	45.6	44.2
PA	3	49.5	48.4	48.9
PA	3	46.2	46.3	46.3
PA	3	45.4	46.1	45.7

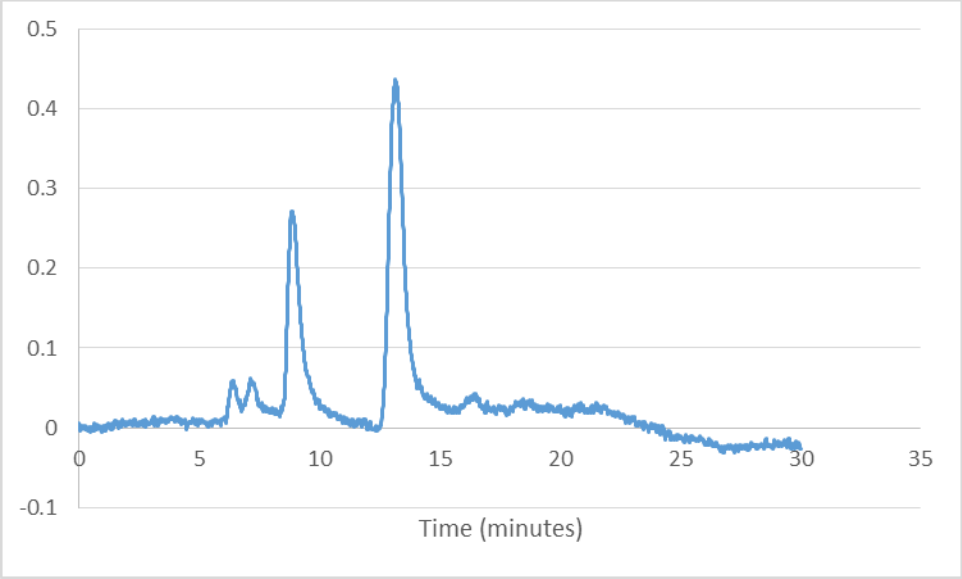

Figure A-1. Control Sample HPLC UV 0-30 minutes

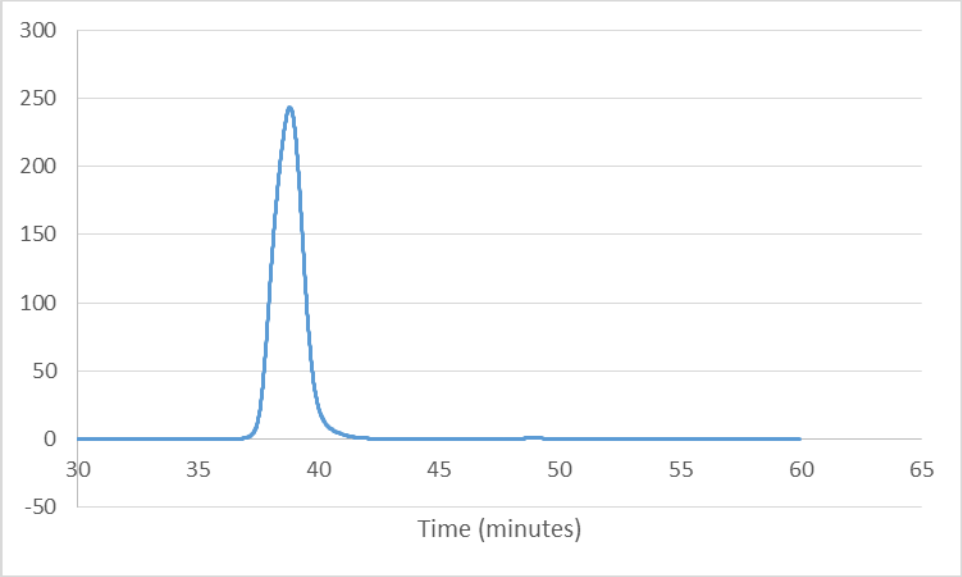

Figure A-2. Control Sample HPLC UV 30-60 minutes

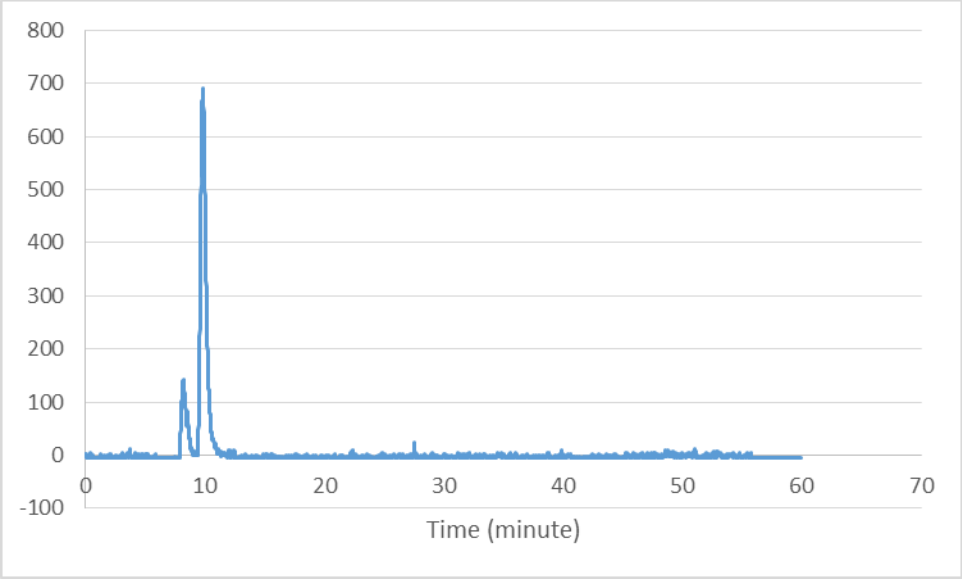

Figure A-3. Control Sample HPLC ESLD results

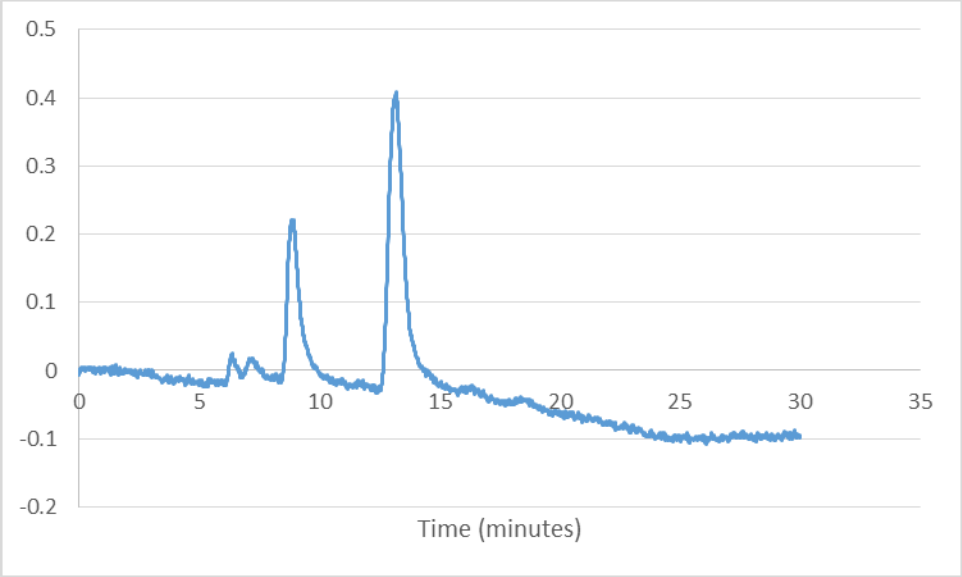

Figure A-4. Polyamide effluent HPLC UV 0-30 minutes

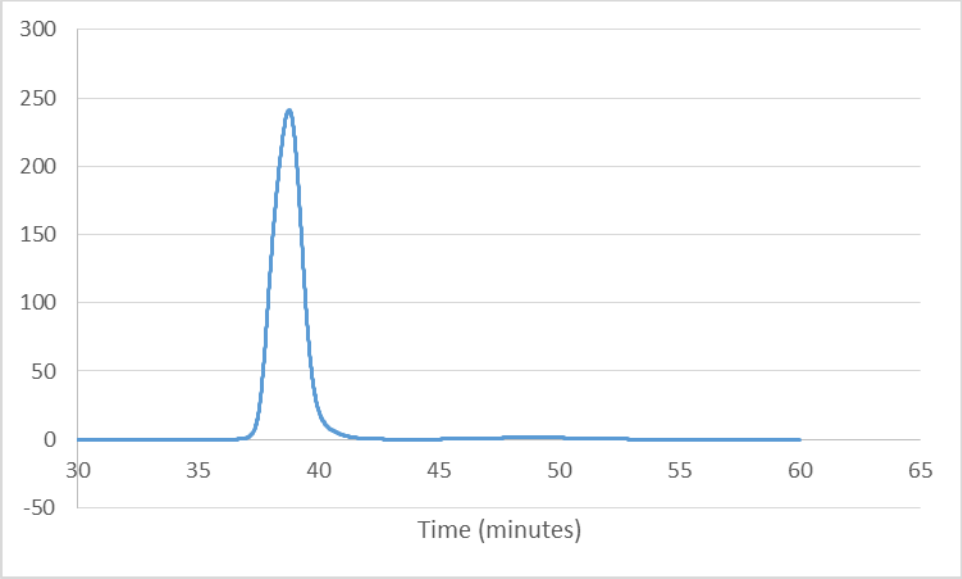

Figure A-5. Polyamide effluent HPLC UV 30-60 minutes

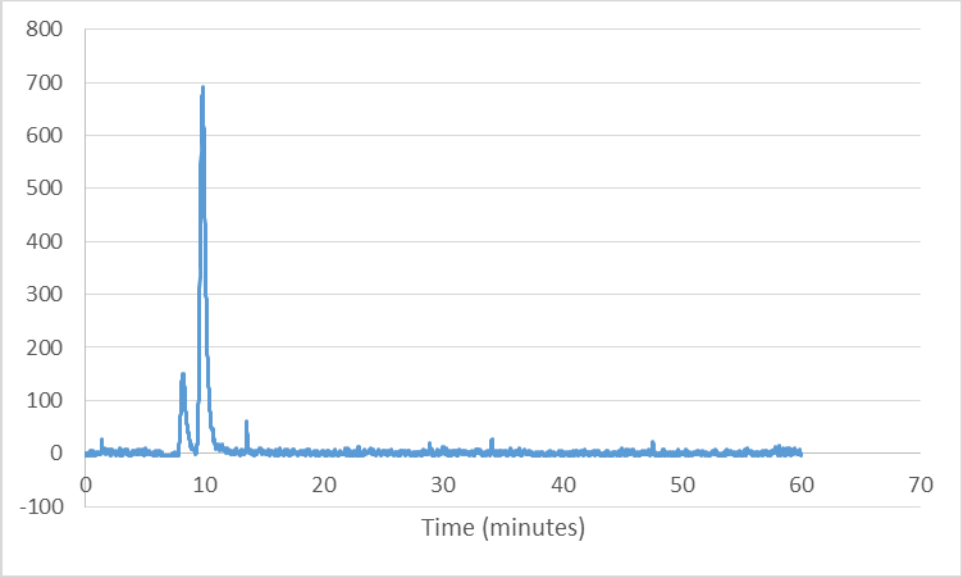

Figure A-6. Polyamide effluent HPLC ESLD results

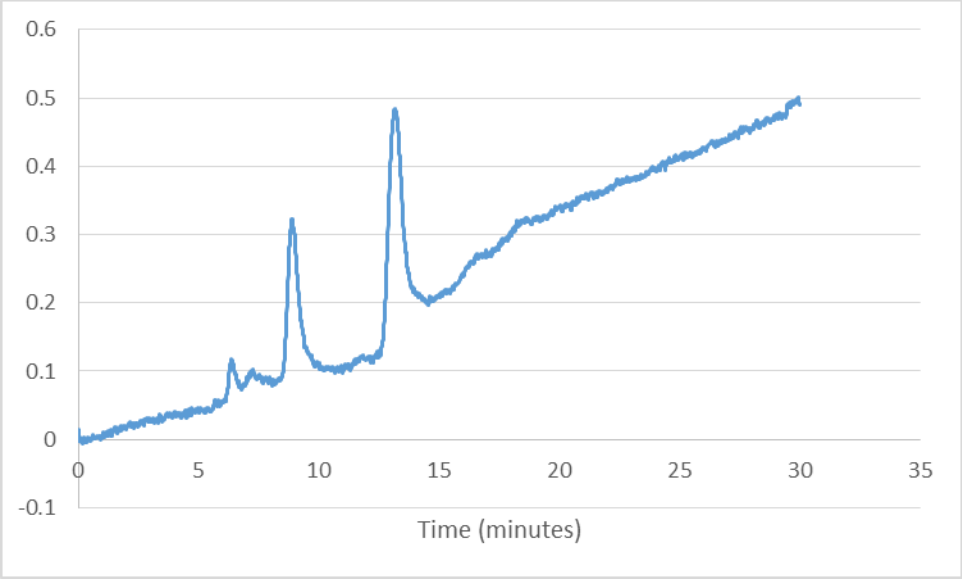

Figure A-7. Polyethersulfone effluent HPLC UV 0-30 minutes

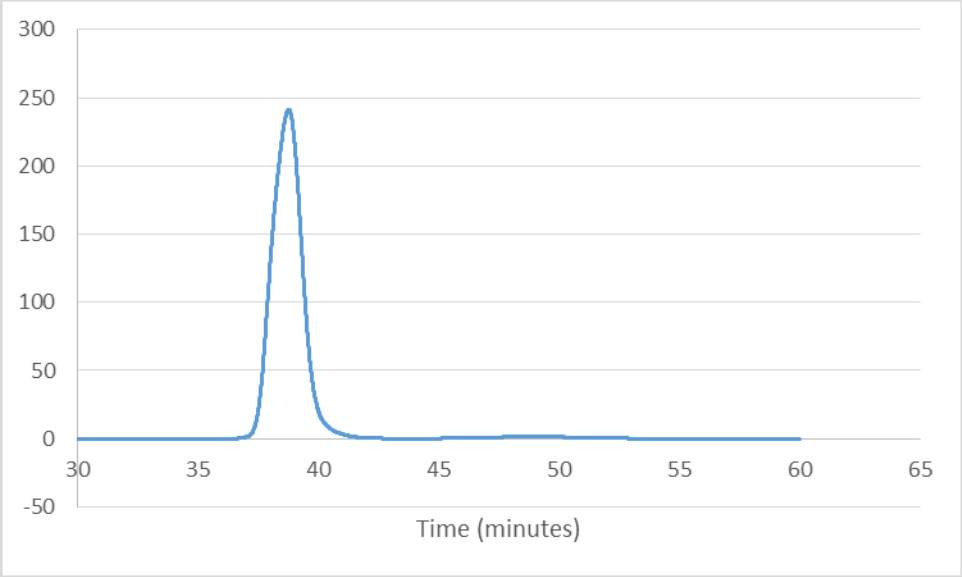

Figure A-8. Polyethersulfone effluent HPLC UV 30-60 minutes

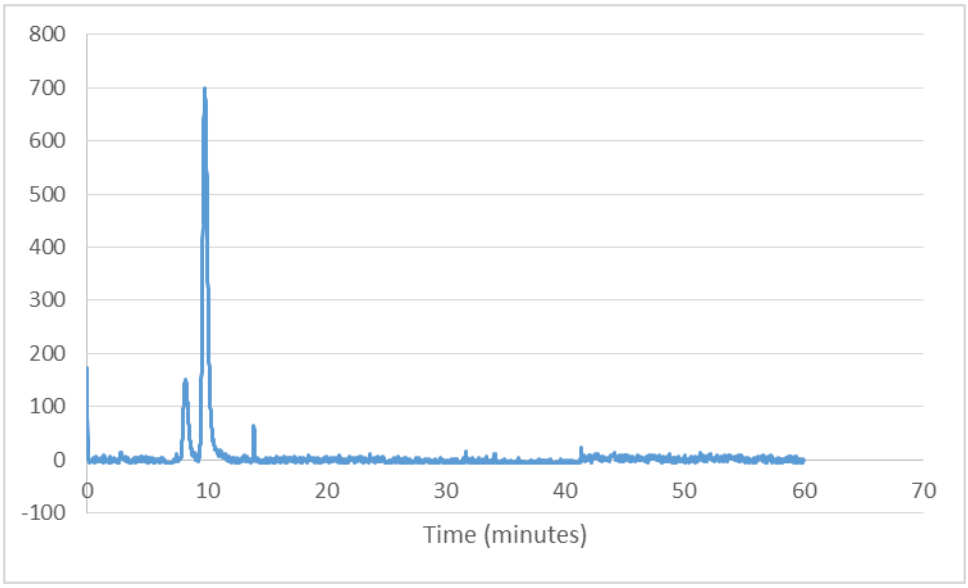

Figure A-9. Polyethersulfone effluent HPLC ESLD results

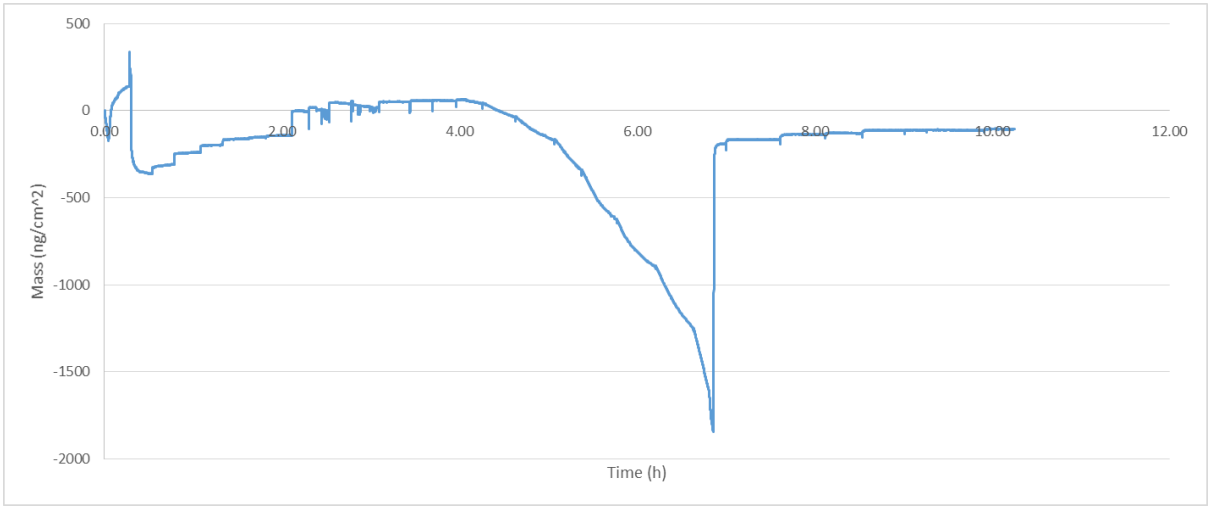

Figure A-10 Polyamide fouling 2/25/15 omitted from report due to poor quality, likely due to a bubble on the sensor

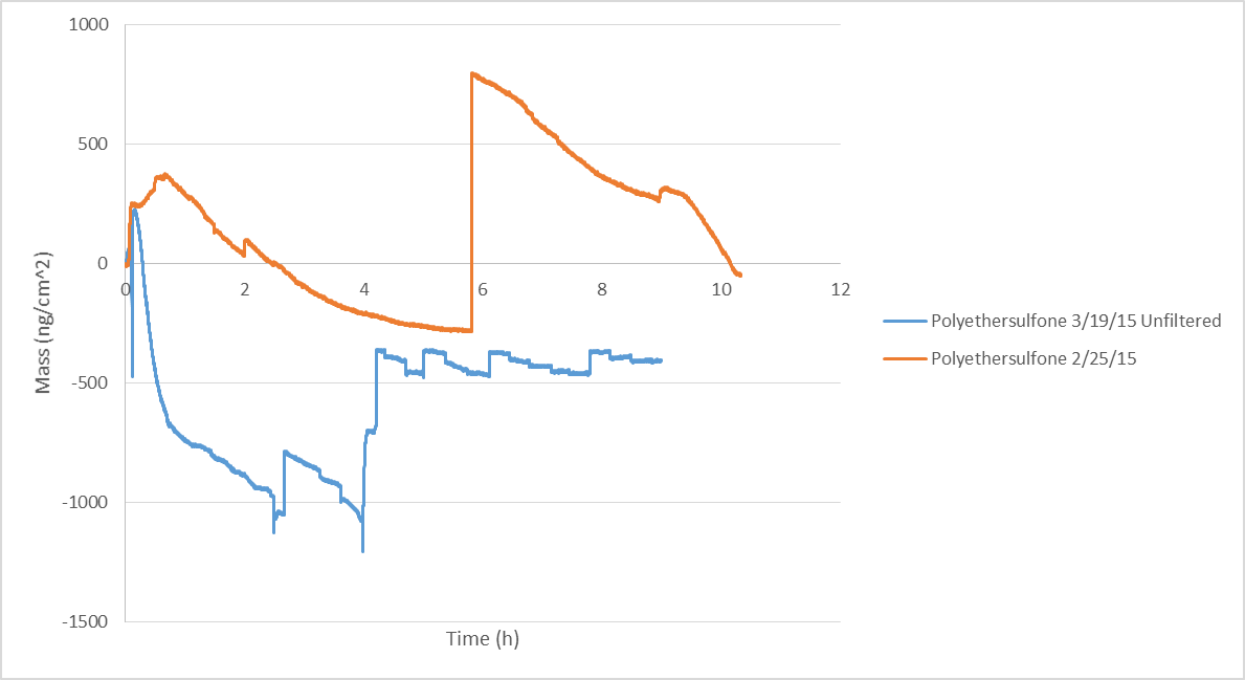

Figure A-11 PES fouling results omitted from the report

Protocol A-I

1. UV/ozone treat for 10 minutes (see UVO treatment).
2. Heat a 5:1:1 mixture of milliQ water, ammonia (25%) and hydrogen peroxide (30%) to 75°C, approx. 10 ml is sufficient.
3. Place the sensor in the heated solution for 5 minutes.
4. Rinse with milliQ water. *It is important that the surfaces are kept wet after ammonium-peroxide immersion until they are rinsed well with water.*
5. Dry with nitrogen gas.
6. UV/ozone treat for 10 minutes (see UVO treatment).

Figure A-12 Cleaning protocol A-1

Protocol UVO

1. Place the sensor surfaces in a UV/ozone chamber, approximately 5 mm from the lamp.
2. Turn on the UV lamp for 5-10 minutes. The time is dependent on the power of the lamp. A minimum of 12 mW/cm^2 at 1 inch from a 185/254 nm lamp is recommended.

Figure A-13 UVO protocol

Protocol Daily

1. Mount a sensor surface into the chamber / flow module(s).
2. Pump approximately 20 ml of 2% Hellmanex II through the system (heating to 30°C could improve the cleaning effect).
3. Pump 100 ml of milliQ water through the system.
4. Empty the chamber / flow module from liquid and dry visible parts with nitrogen gas.

Figure A-14 Cleaning Protocol Daily